Astron. Astrophys. 293, 953–966 (1995)

ASTRONOMY AND ASTROPHYSICS

Atomic data from the Iron Project

VI. Collision strengths and rate coefficients for Fe II*

H.L. Zhang and A.K. Pradhan

Department of Astronomy, Ohio State University, 174 West 18th Avenue, Columbus, OH 43210-1106, USA
Internet: zhang@payne.mps.ohio-state.edu

Received 7 April 1994 / Accepted 13 June 1994

Abstract. Collision strengths and maxwellian averaged rate coefficients have been calculated for 10 011 infrared, optical and ultraviolet transitions among 142 fine structure levels in Fe II. Collision strengths are calculated using the R-matrix method with a 38 term close-coupling target expansion and for electron energies up to 10 rydbergs. Rate coefficients are tabulated at a wide range of temperatures at which Fe II is abundant in plasma sources. A brief discussion of the calculations, sample results, and comparison with earlier works are given. The present rates for Fe II are expected to find applications in the IR, O, and UV spectral diagnostics of astrophysical objects and laboratory fusion plasmas

Key words: atomic data – plasmas – ultraviolet: general – infrared: general

1. Introduction

Fe II emission is observed from nearly all classes of astronomical objects over a wide spectral range from the infrared to the ultraviolet. The relatively low ionization potential of Iron and the rich atomic structure of Fe II combine to ensure that a very large number of transitions occur in astrophysical sources as diverse as extended H II regions or gaseous nebulae, active galactic nuclei, quasars, Seyfert galaxies, supernovae, and the Sun. It has therefore been recognized for a long time that accurate, as well as extensive, atomic data is needed for collisional and radiative processes in Fe II (Viotti et al. 1988). As the first paper of the second phase of the Iron Project that deals with electron impact excitation of fine structure levels in iron ions (Hummer et al. 1993, hereafter Paper I.), we present the final results from an extensive calculation of collision strengths and rate coefficients for Fe II. An accompanying paper by Nahar (1994) reports a large number of transition probabilities for fine structure dipole transitions in Fe II. In an earlier paper, a brief report on the IR line ratios for Fe II using some of the data presented in this work was presented by Pradhan & Zhang (1993).

The complexity of the atomic structure of Fe II places rather a formidable demand on computational resources. As such, few previous results are available and several of these are not accurate. Previous works on Fe II are by Nussbaumer & Storey (NS 1980, 1988) who calculated collision strengths between 4 low-lying LS terms ($3d^6 4s\ a^6D$, $3d^7\ a^4F$, $3d^6 4s\ a^4D$ and $3d^7\ a^4P$) for 3 energies above the thresholds of these terms; Baluja et al. (1986), who carried out a four-state calculation, also in LS coupling; Berrington et al. (1988), who calculated collision strengths between 16 fine structure levels arising from these 4 terms and pointed out that the NS results did not include resonances, and, although the Baluja et al. results did include some resonances, they consisted of a giant pseudo-resonance and therefore were not correct. Keenan et al. (1988) tabulated the maxwellian averaged collision strengths obtained by Berrington et al. (1988) for the 4 lowest LS terms.

To provide accurate data for spectral diagnostics, Pradhan & Berrington (1993, hereafter PB) initiated calculations with a 38-term target expansion for Fe II, using the R-matrix method (Paper I). In that work, they included 38 quartet and sextet terms, dominated by configurations $3d^6 4s$, $3d^7$ and $3d^6 4p$, in the non-relativistic case to obtain collision strengths between these 38 LS terms. In addition, they also included 41 fine structure levels, belonging to 10 quartet and sextet terms, in the relativistic Breit-Pauli (BP) calculations. The PB work however showed some inconsistencies when the BP collision strengths were summed over the fine structure and compared with the LS values, and therefore their fine structure collision strengths may not be accurate.

In the present work, the LS coupling calculations by PB have been extended to include fine structure, using the full 38-term target expansion. The calculations were done with the non-relativistic algebraic recoupling to transform the reactance matrix (the K-matrix) from LS coupling to pair coupling (Eissner et al. 1974), using a revised and optimized version of the STGFJ

Send offprint requests to: A.K. Pradhan

* Tables for complete data for Fe II are only available in electronic form, see the editorial in A&A 1992, Vol. 266 No 2, page E1

Table 1. Observed energies (Ryd) for the 142 fine structure levels in Fe II (Corliss and Sugar 1982)

L	Term		J	Energy	L	Term		J	Energy
1	$3d^6(^5D)4s$	a^6D	9/2	0.00000	41	$3d^6(^5D)4p$	z^6F^o	11/2	0.38244
2			7/2	0.00351	42			9/2	0.38378
3			5/2	0.00608	43			7/2	0.38489
4			3/2	0.00786	44			5/2	0.38578
5			1/2	0.00890	45			3/2	0.38639
6	$3d^7$	a^4F	9/2	0.01706	46			1/2	0.38674
7			7/2	0.02214	47	$3d^6(^5D)4p$	z^6P^o	7/2	0.38873
8			5/2	0.02586	48			5/2	0.39402
9			3/2	0.02841	49			3/2	0.39750
10	$3d^6(^5D)4s$	a^4D	7/2	0.07249	50	$3d^6(^5D)4p$	z^4D^o	7/2	0.40503
11			5/2	0.07647	51			5/2	0.40811
12			3/2	0.07910	52			3/2	0.41047
13			1/2	0.08062	53			1/2	0.41195
14	$3d^7$	a^4P	5/2	0.12279	54	$3d^6(^5D)4p$	z^4F^o	9/2	0.40308
15			3/2	0.12460	55			7/2	0.40783
16			1/2	0.12671	56			5/2	0.41080
17	$3d^6(^3P_2)4s$	b^4P	5/2	0.18982	57			3/2	0.41271
18			3/2	0.19877	58	$3d^6(^5D)4p$	z^4P^o	5/2	0.42800
19			1/2	0.20421	59			3/2	0.43185
20	$3d^6(^3H)4s$	a^4H	13/2	0.19366	60			1/2	0.43400
21			11/2	0.19529	61	$3d^6(^3F_1)4s$	c^4F	9/2	0.45707
22			9/2	0.19667	62			7/2	0.45735
23			7/2	0.19785	63			5/2	0.45693
24	$3d^6(^3F_2)4s$	b^4F	9/2	0.20629	64			3/2	0.45633
25			7/2	0.20786	65	$3d^6(^3P_1)4s$	c^4P	5/2	0.45757
26			5/2	0.20904	66			3/2	0.45114
27			3/2	0.20988	67			1/2	0.44744
28	$3d^6(^3G)4s$	a^4G	11/2	0.23172	68	$3d^6(^3P_2)4p$	z^4S^o	3/2	0.54369
29			9/2	0.23516	69	$3d^6(^3P_2)4p$	y^4P^o	5/2	0.55043
30			7/2	0.23676	70			3/2	0.55891
31			5/2	0.23743	71			1/2	0.55619
32	$3d^6(^3D)4s$	b^4D	7/2	0.28690	72	$3d^6(^3H)4p$	z^4G^o	11/2	0.55246
33			5/2	0.28603	73			9/2	0.55412
34			3/2	0.28581	74			7/2	0.55548
35			1/2	0.28585	75			5/2	0.55625
36	$3d^6(^5D)4p$	z^6D^o	9/2	0.35046	76	$3d^6(^3H)4p$	z^4H^o	13/2	0.55439
37			7/2	0.35230	77			11/2	0.55485
38			5/2	0.35411	78			9/2	0.55578
39			3/2	0.35551	79			7/2	0.55730
40			1/2	0.35639					

code which is an extension of the asymptotic region code, STGF, of the non-relativistic (LS coupling) R-matrix package. We expect this non-relativistic approach to be sufficiently accurate, since the relativistic effects are not very important compared to the electron-electron correlations for Fe II, as pointed out by Berrington et al. (1988) and shown in PB. Another major consideration is that the full BP calculations would be considerably larger and even more time consuming than the present work. PB pointed out in the discussion of their Fig. 6(b), showing the BP results, that the fine structure BP calculations did not seem to be accurate due to an inadequate number of LS terms included in the coupled channel scheme. But, to include all 142 or more fine structure levels in the BP calculations would be a formidable problem in terms of the present computational resources. Therefore, it appears it is more appropriate to include more LS terms in the non-relativistic close-coupling calculations than to include only a few terms in the BP calculations.

In the present work, collision strengths are calculated for all 10 011 transitions between the 142 fine structure levels corresponding to the 38 LS terms in the target expansion for electron

Table 1. (continued)

L	Term		J	Energy	L	Term		J	Energy
80	$3d^6(^3H)4p$	z^4I^o	15/2	0.55904	112	$3d^6(^3D)4p$	w^4P^o	5/2	0.65579
81			13/2	0.56068	113			3/2	0.65650
82			11/2	0.56122	114			1/2	0.65805
83			9/2	0.56054	115	$3d^6(^3D)4p$	w^4D^o	7/2	0.66205
84	$3d^6(^3P_2)4p$	y^4D^o	7/2	0.56249	116			5/2	0.66176
85			5/2	0.57127	117			3/2	0.66089
86			3/2	0.57375	118			1/2	0.66003
87			1/2	0.57254	119	$3d^6(^3D)4p$	w^4F^o	9/2	0.66204
88	$3d^6(^3F_2)4p$	x^4D^o	7/2	0.57360	120			7/2	0.65932
89			5/2	0.57659	121			5/2	0.65829
90			3/2	0.57834	122			3/2	0.65765
91			1/2	0.57920	123	$3d^6(^3P_1)4p$	v^4D^o	7/2	0.79216
92	$3d^6(^3F_2)4p$	y^4F^o	9/2	0.56643	124			5/2	0.79068
93			7/2	0.56558	125			3/2	0.78865
94			5/2	0.56637	126			1/2	0.78723
95			3/2	0.56721	127	$3d^6(^3F_1)4p$	$^4G^o$	11/2	0.82207
96	$3d^6(^3F_2)4p$	y^4G^o	11/2	0.58208	128			9/2	0.82053
97			9/2	0.58274	129			7/2	0.81914
98			7/2	0.58358	130			5/2	0.81766
99			5/2	0.58401	131	$3d^6(^3P_1)4p$	$^4S^o$	3/2	0.82588
100	$3d^6(^3G)4p$	x^4F^o	9/2	0.60155	132	$3d^6(^3P_1)4p$	$^4P^o$	5/2	0.84086
101			7/2	0.60487	133			3/2	0.82833
102			5/2	0.60620	134			1/2	0.82779
103			3/2	0.60702	135	$3d^6(^3F_1)4p$	$^4D^o$	7/2	0.84866
104	$3d^6(^3G)4p$	x^4G^o	11/2	0.59761	136			5/2	0.84656
105			9/2	0.59867	137			3/2	0.84427
106			7/2	0.60081	138			1/2	0.84250
107			5/2	0.60215	139	$3d^6(^3F_1)4p$	u^4F^o	9/2	0.85189
108	$3d^6(^3G)4p$	y^4H^o	13/2	0.60519	140			7/2	0.85192
109			11/2	0.60566	141			5/2	0.85108
110			9/2	0.60680	142			3/2	0.85047
111			7/2	0.60756					

energy range 0 to 10 rydbergs. The maxwellian averaged rate coefficients or effective collision strengths, Υ, are also calculated and tabulated for temperature range 1000 to 100 000 K. This is expected to cover the temperatures at which Fe II is most abundant in most astrophysical sources.

A brief description of the computations, the results, and a comparison with earlier works by NS (1980, 1988), Keenan et al. (1988) and PB are given in the following sections.

2. Atomic calculations

2.1. Target data

As mentioned above, the target expansion for the present calculations is the same as that in PB, that is, the target states chosen consisted of the 38 sextet and quartet symmetries dominated by the configurations $3d^64s$, $3d^7$ and $3d^64p$. The doublet symmetries and states dominated by other configurations were omitted. The 38 LS terms and their observed term energies are tabulated in Table 1 of PB.

For convenience, the 142 fine structure levels formed by these 38 terms, and their observed energies (Corliss & Sugar 1982), are listed in Table 1.

2.2. Collision strengths: calculations

The collision strengths were calculated for a large number of electron energies ranging from 0 to 10 rydbergs. The choice of the energy range is made carefully in order to obtain detailed collision strengths in the region where they are dominated by resonances, as well as in an extended region where resonances are not important or have not been included but which is necessary for an accurate calculation of the maxwellian averaged values, particularly for dipole allowed transitions. Of primary importance are the IR, O, and UV transitions in Fe II that cor-

respond to a number of the low-lying levels of configurations $3d^6 4s$, $3d^7$, and $3d^6 4p$.

In order to delineate the resonance structures, an effective quantum number mesh (ν-mesh) was used to obtain the collision strengths at 2699 energy points in the range $E = 0 - 0.55$ rydbergs. The advantage of a mesh with a constant interval in effective quantum number $\nu = z/\sqrt{|E|}$, vs. a constant energy interval, is that the resonances corresponding to increasing values of ν become narrower in energy but are still resolved with the same precision (see Paper I). However, the calculations need to be carried out at a large number of energies. In the present calculations the range of energies from 0 to 0.55 rydbergs was covered by 2699 energies corresponding to the ν-mesh. This mesh and this energy range not only yield detailed resonance structures for transitions between the levels of low-lying terms, such as a^6D, a^4F, a^4D and a^4P, but also for transitions from these levels to higher levels. The near threshold resonance structures in the collision strengths for optically allowed transitions, namely for transitions from the levels of the lower even-parity levels of $3d^6 4s$ and $3d^7$ to the odd-parity levels of the terms dominated by $3d^6 4p$, such as z^6F^o, z^6D^o and z^6P^o, as well as to several of the quartet odd-parity levels, are also resolved.

In the higher energy region $E > 0.55$ rydbergs, the collision strengths were calculated for 101 additional energy points up to 10 rydbergs. The fine $\nu-$mesh up to $E = 0.55$ accounts for the most important resonance features in the excitation of low-lying levels of a^6D, a^4F, a^4D and a^4P terms, not only arising from coupling with z^6D^o, z^4F^o and z^4P^o terms, but also from coupling with higher odd parity terms, such as z^4S^o, y^4P^o, z^4G^o, z^4H^o, and z^4I^o. A practical reason for terminating the $\nu-$mesh at 0.55 rydbergs is that it would take considerably more computing time and memory resources, owing to a large number of additional channels that become open with higher energies. When channels associated with the high-lying odd parity terms with $E > 0.55$ rydbergs are open, the resonances for excitation to levels of these terms are not important, since most transitions are optically allowed.

As is well known, for low impact electron energies, contributions to the collision strength from small $J\pi$ total symmetries are dominant and those from large symmetries are negligible, especially for the forbidden transitions between the low-lying levels in the Fe II case. Therefore, for $E = 0$–0.349 rydbergs, that is when all transition channels to the levels of the odd-parity terms, z^6F^o, z^6D^o and z^6P^o, are closed, we calculated partial wave contributions from total angular momenta of the electron plus target system $J = 0$–6 (where $\boldsymbol{J} = \boldsymbol{L}+\boldsymbol{S}$; $\boldsymbol{L}$ and $\boldsymbol{S}$ are total orbital and spin angular momenta). We consider the recoupling of 60 $SL\pi$ symmetries described in Sect. 3 of PB. For higher energies $E > 0.349$, 18 additional $SL\pi$'s are included with

$$10 \leq L \leq 13$$

$$(2S+1) = 3, 5, 7$$

$$\pi = \text{even and odd},$$

and collision strengths were calculated for J up to 10. Test results show that contributions by $J = 7$–10 for the forbidden transitions between the low-lying levels dominated by configurations $3d^6 4s$ and $3d^7$ are indeed negligible, while their contribution to the optically allowed transitions are pronounced but not dominant.

Owing to the long-range nature of the Coulomb potential, the dominant contribution to dipole allowed transitions arises from high partial waves. In the close-coupling scattering calculations it is necessary to consider low partial waves that involve close interactions with the target ion. Present calculations include $l \leq 9$ in the R-matrix calculations. However, at large impact parameters associated with higher partial waves simpler approximations may be employed. The procedure is referred to as "top-up" (Paper I). The Coulomb-Bethe approximation was employed for "top-up" in l at energies greater than 0.349 rydbergs where $l > 9$ are expected to contribute. The Coulomb Bethe approximation requires dipole oscillator strengths for the corresponding transitions. The data for the oscillator strengths for a large number of fine structure dipole transitions has been obtained by Nahar (1994). (The accompanying paper by Nahar in this issue reports 21 587 transition probabilities for dipole fine structure transitions in Fe II, obtained as an extension of the work for the Opacity Project by Nahar & Pradhan 1994). These oscillator strengths from Nahar (1994) were used as input to the Coulomb-Bethe calculations for all dipole allowed transitions in the present work.

It is necessary to exercise some care in the top-up procedure to match the low and the high partial wave contributions to allowed transitions. The contributions to the total collision strength are organized according to the total $J\pi$'s in the code STGFJ. However, the high partial wave contributions are estimated in terms of the free electron orbitals l's in the Coulomb-Bethe approximation; therefore a choice of $l_{\rm min}$ as the lowest value in the Coulomb-Bethe approximation is somewhat ambiguous but may be estimated from the distance of closest approach at a given energy and ion charge (Seaton 1975). The procedure that we use is as follows: first, we obtain collision strengths for the optically allowed transitions between the LS terms, with top-up in l in LS coupling; second, we calculate and match the calculated collision strengths, obtained by using the Coulomb-Bethe approximation with different starting $l_{\rm min}$ values and summed over the fine structure, with the total LS values. It is found that $l_{\rm min} = 9$ provides the best match, that is by adding partial wave contributions with $9 \leq l \leq \infty$ from the Coulomb-Bethe approximation to the collision strengths obtained by detailed calculations we obtain values close to those in LS coupling.

2.3. *Collision strengths: results*

In this subsection we compare the present collision strength results with those by earlier works, mainly by PB and by NS (1980). While it is seen that the present results are similar to the 38-term LS results of the PB work, since the target expansion is the same, they are different from the 41-level BP results in that work. It is also found that the resonance and coupling effects are very important and should dominate over the relativistic effects

Table 2. Transition keys for ϒ's in Table 3–6 for Fe II. The level indices are referred to Table 1

1	17	1	18	1	19	1	20	1	21	1	22	1	23	1	24	1	25	1	26
1	27	1	28	1	29	1	30	1	31	1	32	1	33	1	34	1	35	1	36
1	37	1	38	1	39	1	40	1	41	1	42	1	43	1	44	1	45	1	46
1	47	1	48	1	49	1	50	1	51	1	52	1	53	1	54	1	55	1	56
1	57	1	58	1	59	1	60	1	61	1	62	1	63	1	64	1	65	1	66
1	67	2	17	2	18	2	19	2	20	2	21	2	22	2	23	2	24	2	25
2	26	2	27	2	28	2	29	2	30	2	31	2	32	2	33	2	34	2	35
2	36	2	37	2	38	2	39	2	40	2	41	2	42	2	43	2	44	2	45
2	46	2	47	2	48	2	49	2	50	2	51	2	52	2	53	2	54	2	55
2	56	2	57	2	58	2	59	2	60	2	61	2	62	2	63	2	64	2	65
2	66	2	67	3	17	3	18	3	19	3	20	3	21	3	22	3	23	3	24
3	25	3	26	3	27	3	28	3	29	3	30	3	31	3	32	3	33	3	34
3	35	3	36	3	37	3	38	3	39	3	40	3	41	3	42	3	43	3	44
3	45	3	46	3	47	3	48	3	49	3	50	3	51	3	52	3	53	3	54
3	55	3	56	3	57	3	58	3	59	3	60	3	61	3	62	3	63	3	64
3	65	3	66	3	67	4	17	4	18	4	19	4	20	4	21	4	22	4	23
4	24	4	25	4	26	4	27	4	28	4	29	4	30	4	31	4	32	4	33
4	34	4	35	4	36	4	37	4	38	4	39	4	40	4	41	4	42	4	43
4	44	4	45	4	46	4	47	4	48	4	49	4	50	4	51	4	52	4	53
4	54	4	55	4	56	4	57	4	58	4	59	4	60	4	61	4	62	4	63
4	64	4	65	4	66	4	67	5	17	5	18	5	19	5	20	5	21	5	22
5	23	5	24	5	25	5	26	5	27	5	28	5	29	5	30	5	31	5	32
5	33	5	34	5	35	5	36	5	37	5	38	5	39	5	40	5	41	5	42
5	43	5	44	5	45	5	46	5	47	5	48	5	49	5	50	5	51	5	52
5	53	5	54	5	55	5	56	5	57	5	58	5	59	5	60	5	61	5	62
5	63	5	64	5	65	5	66	5	67	6	17	6	18	6	19	6	20	6	21
6	22	6	23	6	24	6	25	6	26	6	27	6	28	6	29	6	30	6	31
6	32	6	33	6	34	6	35	6	36	6	37	6	38	6	39	6	40	6	41
6	42	6	43	6	44	6	45	6	46	6	47	6	48	6	49	7	17	7	18
7	19	7	20	7	21	7	22	7	23	7	24	7	25	7	26	7	27	7	28
7	29	7	30	7	31	7	32	7	33	7	34	7	35	7	36	7	37	7	38
7	39	7	40	7	41	7	42	7	43	7	44	7	45	7	46	7	47	7	48
7	49	8	17	8	18	8	19	8	20	8	21	8	22	8	23	8	24	8	25
8	26	8	27	8	28	8	29	8	30	8	31	8	32	8	33	8	34	8	35
8	36	8	37	8	38	8	39	8	40	8	41	8	42	8	43	8	44	8	45
8	46	8	47	8	48	8	49	9	17	9	18	9	19	9	20	9	21	9	22
9	23	9	24	9	25	9	26	9	27	9	28	9	29	9	30	9	31	9	32
9	33	9	34	9	35	9	36	9	37	9	38	9	39	9	40	9	41	9	42
9	43	9	44	9	45	9	46	9	47	9	48	9	49	10	17	10	18	10	19
10	20	10	21	10	22	10	23	10	24	10	25	10	26	10	27	10	28	10	29
10	30	10	31	10	32	10	33	10	34	10	35	10	36	10	37	10	38	10	39
10	40	10	41	10	42	10	43	10	44	10	45	10	46	10	47	10	48	10	49
11	17	11	18	11	19	11	20	11	21	11	22	11	23	11	24	11	25	11	26
11	27	11	28	11	29	11	30	11	31	11	32	11	33	11	34	11	35	11	36
11	37	11	38	11	39	11	40	11	41	11	42	11	43	11	44	11	45	11	46
11	47	11	48	11	49	12	17	12	18	12	19	12	20	12	21	12	22	12	23
12	24	12	25	12	26	12	27	12	28	12	29	12	30	12	31	12	32	12	33
12	34	12	35	12	36	12	37	12	38	12	39	12	40	12	41	12	42	12	43
12	44	12	45	12	46	12	47	12	48	12	49	13	17	13	18	13	19	13	20
13	21	13	22	13	23	13	24	13	25	13	26	13	27	13	28	13	29	13	30
13	31	13	32	13	33	13	34	13	35	13	36	13	37	13	38	13	39	13	40
13	41	13	42	13	43	13	44	13	45	13	46	13	47	13	48	13	49	14	17
14	18	14	19	14	20	14	21	14	22	14	23	14	24	14	25	14	26	14	27
14	28	14	29	14	30	14	31	14	32	14	33	14	34	14	35	14	36	14	37
14	38	14	39	14	40	14	41	14	42	14	43	14	44	14	45	14	46	14	47
14	48	14	49	15	17	15	18	15	19	15	20	15	21	15	22	15	23	15	24
15	25	15	26	15	27	15	28	15	29	15	30	15	31	15	32	15	33	15	34
15	35	15	36	15	37	15	38	15	39	15	40	15	41	15	42	15	43	15	44
15	45	15	46	15	47	15	48	15	49	16	17	16	18	16	19	16	20	16	21
16	22	16	23	16	24	16	25	16	26	16	27	16	28	16	29	16	30	16	31
16	32	16	33	16	34	16	35	16	36	16	37	16	38	16	39	16	40	16	41
16	42	16	43	16	44	16	45	16	46	16	47	16	48	16	49				

Table 3. Maxwellian-averaged collision strengths Υ at T = 5000 K in Fe II

3.30E-1	1.08E-1	7.43E-3	6.49E-1	3.19E-1	9.62E-2	1.61E-2	3.65E-1	2.15E-1	1.11E-1
3.70E-2	2.44E-1	2.07E-1	7.78E-2	1.99E-2	2.62E-1	1.50E-1	7.01E-2	3.55E-2	2.13E+1
7.81E+0	1.54E+0	7.08E-1	2.77E-1	2.94E+1	5.19E+0	6.53E-1	9.37E-2	3.73E-2	1.63E-2
1.18E+1	2.11E-1	4.95E-2	1.50E+0	2.75E-1	1.42E-2	2.68E-3	2.49E+0	3.21E-1	3.44E-2
1.07E-2	8.70E-1	1.70E-2	9.27E-3	1.22E-1	8.57E-2	3.71E-2	9.08E-3	7.22E-2	4.62E-2
1.82E-2	1.92E-1	1.04E-1	6.20E-2	2.85E-1	2.37E-1	2.49E-1	1.00E-1	2.00E-1	2.23E-1
1.03E-1	9.30E-2	1.19E-1	2.06E-1	1.39E-1	7.52E-2	1.64E-1	1.35E-1	1.02E-1	2.72E-2
6.14E+0	1.10E+1	8.55E+0	1.31E+0	4.85E-1	7.41E-1	1.92E+1	6.94E+0	1.18E+0	1.18E-1
2.30E-2	3.50E+0	5.97E+0	1.30E-1	5.00E-1	6.62E-1	2.57E-1	1.16E-2	4.88E-1	1.44E+0
3.25E-1	2.96E-2	3.31E-1	3.80E-1	6.46E-3	8.68E-2	3.71E-2	4.45E-2	3.43E-2	5.65E-2
3.23E-2	2.04E-2	9.62E-2	1.03E-1	7.06E-2	8.00E-2	2.16E-1	1.60E-1	1.99E-1	1.18E-1
1.22E-1	1.61E-1	8.14E-2	6.52E-2	1.36E-1	1.43E-1	1.12E-1	9.80E-2	1.19E-1	6.37E-2
4.74E-2	8.98E-1	8.11E+0	4.14E+0	7.32E+0	8.20E-1	1.11E-1	7.23E-1	1.19E+1	6.75E+0
1.45E+0	1.15E-1	6.80E-1	4.28E+0	2.24E+0	1.26E-1	4.57E-1	3.40E-1	1.47E-1	6.51E-2
5.80E-1	8.61E-1	2.08E-1	1.07E-1	3.08E-1	1.23E-1	4.37E-2	4.05E-2	3.19E-2	3.60E-2
3.98E-2	2.64E-2	1.57E-2	3.93E-2	8.53E-2	5.49E-2	1.15E-2	1.05E-1	1.39E-1	1.82E-1
5.35E-2	8.21E-2	1.08E-1	7.99E-2	2.26E-2	7.10E-2	1.06E-1	1.12E-1	5.81E-2	6.90E-2
5.52E-2	3.78E-2	3.34E-1	1.17E+0	7.00E+0	1.21E+0	4.56E+0	4.21E-2	1.01E-1	5.13E-1
6.73E+0	5.38E+0	1.28E+0	6.12E-2	1.48E+0	3.27E+0	2.10E-2	1.78E-1	2.87E-1	2.12E-1
1.16E-2	9.83E-2	5.06E-1	5.01E-1	2.93E-2	1.49E-1	1.81E-1	1.58E-2	3.50E-2	2.91E-2
2.15E-2	2.47E-2	2.03E-2	9.60E-3	1.18E-2	4.85E-2	2.92E-2	5.95E-4	1.84E-2	1.01E-1
9.85E-2	1.61E-2	5.26E-2	3.74E-2	5.58E-2	4.33E-3	2.83E-2	5.34E-2	6.96E-2	2.84E-2
2.48E-2	4.00E-2	1.71E-2	9.15E-2	4.84E-1	8.19E-1	4.55E+0	1.42E+0	1.93E-2	1.97E-2
6.42E-2	2.92E-1	3.05E+0	3.58E+0	1.98E-2	6.77E-2	2.31E+0	2.85E-3	3.26E-2	1.63E-1
1.50E-1	5.20E-3	6.45E-3	9.68E-2	4.47E-1	7.13E-3	4.36E-2	1.29E-1	3.58E-3	1.90E-2
2.04E-2	7.73E-3	1.17E-2	1.13E-2	4.32E-3	5.79E-1	1.08E-1	2.76E-2	1.03E+0	4.05E-1
8.53E-2	1.05E-2	1.06E+0	3.44E-1	9.22E-2	1.27E-2	6.45E-1	3.19E-1	9.13E-2	1.33E-2
3.29E-1	2.14E-1	7.65E-2	2.10E-2	8.81E-1	4.32E-1	1.56E-1	5.12E-2	1.30E-2	7.96E-1
4.03E-1	1.76E-1	6.31E-2	1.84E-2	4.11E-3	3.51E-1	1.41E-1	3.01E-2	2.64E-1	2.52E-1
5.71E-2	2.93E-1	5.21E-1	4.46E-1	1.02E-1	3.21E-1	6.10E-1	3.05E-1	1.03E-1	2.40E-1
3.67E-1	2.81E-1	1.06E-1	1.79E-1	2.22E-1	1.29E-1	5.82E-2	3.04E-1	5.50E-1	3.25E-1
1.48E-1	5.68E-2	2.96E-1	3.06E-1	2.70E-1	1.80E-1	8.96E-2	3.03E-2	1.87E-1	1.35E-1
9.45E-2	1.12E-1	2.00E-1	1.17E-1	1.87E-2	3.41E-1	3.22E-1	3.73E-1	8.25E-2	2.87E-1
4.39E-1	2.44E-1	5.60E-2	2.29E-1	2.58E-1	2.38E-1	9.65E-2	1.60E-1	1.46E-1	7.62E-2
1.06E-1	2.63E-1	3.54E-1	2.51E-1	1.07E-1	6.58E-2	2.10E-1	2.00E-1	1.75E-1	1.42E-1
8.27E-2	8.34E-2	1.20E-1	1.08E-1	4.59E-2	1.08E-1	1.32E-1	2.35E-3	1.98E-2	2.67E-1
4.24E-1	1.19E-2	1.00E-1	2.43E-1	3.61E-1	5.04E-3	6.72E-2	1.92E-1	2.51E-1	4.11E-2
9.97E-2	1.11E-1	7.61E-2	2.98E-2	1.11E-1	1.87E-1	2.27E-1	1.60E-1	9.90E-3	5.81E-2
1.37E-1	1.63E-1	1.37E-1	7.59E-2	2.75E-2	9.07E-2	8.90E-2	2.88E-1	1.23E-1	2.82E-2
5.68E-1	2.98E-1	1.34E-1	3.64E-2	3.72E-1	2.01E-1	9.95E-2	4.66E-2	4.82E-1	2.69E-1
1.23E-1	4.62E-2	4.01E-1	3.03E-1	1.73E-1	6.68E-2	3.11E+0	1.66E+0	5.53E-1	1.63E-1
4.63E-2	5.28E+0	1.85E+0	5.88E-1	1.78E-1	5.81E-2	1.98E-2	2.33E+0	3.69E-1	5.78E-2
1.62E-1	9.85E-2	7.00E-2	2.00E-1	2.42E-1	1.90E-1	1.52E-1	1.71E-1	1.65E-1	1.30E-1
7.62E-2	1.87E-1	2.37E-1	1.81E-1	1.22E-1	2.42E-1	3.04E-1	1.59E-1	8.30E-2	8.09E-1
1.80E+0	1.34E+0	6.32E-1	1.74E-1	3.09E-1	2.65E+0	1.85E+0	8.33E-1	2.75E-1	6.76E-2
5.99E-1	1.20E+0	2.73E-1	7.41E-2	8.94E-2	5.67E-2	5.24E-2	1.15E-1	1.86E-1	1.69E-1
7.08E-2	1.08E-1	9.85E-2	8.55E-2	6.31E-2	1.23E-1	1.64E-1	1.43E-1	1.45E-1	1.59E-1
1.73E-1	6.52E-2	1.77E-1	8.65E-1	9.60E-1	8.20E-1	4.86E-1	8.08E-2	1.97E-1	1.26E+0
1.35E+0	8.09E-1	2.91E-1	1.13E-1	6.11E-1	6.49E-1	2.53E-2	5.60E-2	2.88E-2	5.28E-4
5.75E-2	8.44E-2	1.19E-1	2.58E-2	4.37E-2	6.10E-2	5.12E-2	1.28E-2	5.26E-2	8.02E-2
1.00E-1	6.65E-2	8.30E-2	6.52E-2	6.06E-2	4.87E-2	1.35E-1	5.01E-1	5.90E-1	3.77E-1
2.36E-2	5.05E-2	1.04E-1	4.91E-1	7.57E-1	5.63E-1	2.19E-2	1.23E-1	5.34E-1	3.65E+0
2.42E-1	9.35E-2	6.16E-2	3.41E-2	1.83E-2	9.81E-3	4.57E-1	2.31E-1	1.07E-1	4.65E-2
1.22E-1	8.73E-2	5.06E-2	2.48E-2	7.03E-1	4.98E-1	2.60E-1	8.99E-2	5.37E-1	4.18E-1
2.41E-1	1.20E-1	4.69E-2	4.63E-1	3.55E-1	2.34E-1	1.32E-1	6.18E-2	2.17E-2	3.77E-1
2.31E-1	7.71E-2	2.42E-1	2.30E+0	1.13E-1	1.28E-2	2.74E-2	2.55E-2	1.73E-2	1.02E-1
2.06E-1	1.67E-1	9.43E-2	5.44E-2	4.64E-2	4.84E-2	4.78E-2	3.94E-1	3.03E-1	2.59E-1
1.59E-1	2.38E-1	2.26E-1	2.11E-1	1.73E-1	9.69E-2	2.54E-1	1.21E-1	1.19E-1	1.40E-1
1.31E-1	7.83E-2	1.97E-1	8.87E-2	1.70E-1	9.32E-2	1.13E-1	1.12E+0	4.07E-3	6.40E-3
1.28E-2	1.79E-2	2.87E-2	5.45E-2	9.62E-2	1.05E-1	1.01E-2	3.05E-2	3.25E-2	2.60E-2
9.41E-2	2.02E-1	1.55E-1	7.62E-2	5.42E-2	1.43E-1	1.37E-1	9.82E-2	4.94E-2	7.29E-3
1.28E-1	1.30E-1	9.00E-2	4.77E-2	1.84E-2	3.54E-2	1.37E-1	5.62E-2		

Table 4. Maxwellian-averaged collision strengths Υ at T = 10 000 K in Fe II

3.08E-1	9.92E-2	7.99E-3	6.31E-1	3.11E-1	9.51E-2	1.65E-2	4.02E-1	2.15E-1	1.12E-1
3.82E-2	3.44E-1	2.15E-1	7.98E-2	1.98E-2	2.76E-1	1.54E-1	7.31E-2	3.69E-2	2.30E+1
7.06E+0	9.60E-1	4.08E-1	1.55E-1	2.96E+1	5.13E+0	6.00E-1	7.27E-2	2.94E-2	1.32E-2
1.24E+1	1.93E-1	4.55E-2	1.45E+0	2.64E-1	1.22E-2	2.38E-3	2.39E+0	3.06E-1	3.26E-2
1.04E-2	8.58E-1	1.63E-2	8.78E-3	1.29E-1	9.23E-2	4.01E-2	9.71E-3	7.55E-2	4.90E-2
1.97E-2	1.78E-1	9.91E-2	5.64E-2	2.79E-1	2.28E-1	2.42E-1	9.90E-2	2.13E-1	2.26E-1
1.03E-1	9.39E-2	1.55E-1	2.18E-1	1.46E-1	7.75E-2	1.72E-1	1.37E-1	1.05E-1	2.82E-2
6.10E+0	1.11E+1	8.30E+0	8.72E-1	2.91E-1	6.14E-1	1.95E+1	6.98E+0	1.14E+0	9.13E-2
1.69E-2	3.68E+0	6.32E+0	1.20E-1	4.84E-1	6.43E-1	2.50E-1	9.93E-3	4.66E-1	1.38E+0
3.10E-1	2.78E-2	3.26E-1	3.74E-1	6.24E-3	9.35E-2	3.89E-2	4.76E-2	3.72E-2	5.95E-2
3.43E-2	2.15E-2	8.92E-2	9.63E-2	6.50E-2	7.93E-2	2.10E-1	1.55E-1	1.94E-1	1.21E-1
1.22E-1	1.63E-1	8.09E-2	7.08E-2	1.42E-1	1.51E-1	1.18E-1	1.03E-1	1.21E-1	6.44E-2
4.83E-2	6.09E-1	8.02E+0	3.88E+0	7.27E+0	5.74E-1	8.07E-2	6.20E-1	1.22E+1	6.85E+0
1.43E+0	9.05E-2	7.01E-1	4.52E+0	2.36E+0	1.20E-1	4.45E-1	3.29E-1	1.44E-1	6.16E-2
5.55E-1	8.26E-1	1.98E-1	1.05E-1	3.03E-1	1.21E-1	4.72E-2	4.31E-2	3.38E-2	3.87E-2
4.23E-2	2.78E-2	1.64E-2	3.69E-2	7.86E-2	5.14E-2	1.19E-2	1.03E-1	1.35E-1	1.76E-1
5.48E-2	8.22E-2	1.09E-1	8.00E-2	2.26E-2	7.36E-2	1.11E-1	1.18E-1	6.07E-2	7.10E-2
5.58E-2	3.80E-2	2.07E-1	7.87E-1	7.08E+0	9.52E-1	4.61E+0	3.35E-2	6.98E-2	4.48E-1
6.86E+0	5.48E+0	1.27E+0	5.62E-2	1.55E+0	3.45E+0	1.95E-2	1.74E-1	2.82E-1	2.08E-1
1.12E-2	9.31E-2	4.89E-1	4.85E-1	2.85E-2	1.46E-1	1.78E-1	1.70E-2	3.77E-2	3.11E-2
2.28E-2	2.64E-2	2.13E-2	9.97E-3	1.14E-2	4.42E-2	2.76E-2	8.08E-4	1.85E-2	9.86E-2
9.47E-2	1.68E-2	5.31E-2	3.68E-2	5.65E-2	4.13E-3	2.90E-2	5.58E-2	7.39E-2	2.96E-2
2.56E-2	4.07E-2	1.69E-2	5.73E-2	2.90E-1	5.73E-1	4.60E+0	1.43E+0	1.56E-2	1.54E-2
4.32E-2	2.52E-1	3.09E+0	3.67E+0	1.82E-2	6.22E-2	2.45E+0	2.50E-3	3.10E-2	1.60E-1
1.47E-1	5.11E-3	5.91E-3	9.26E-2	4.34E-1	6.84E-3	4.30E-2	1.27E-1	3.79E-3	2.06E-2
2.19E-2	7.98E-3	1.26E-2	1.18E-2	4.47E-3	5.82E-1	1.14E-1	2.84E-2	1.13E+0	4.25E-1
9.48E-2	1.42E-2	1.21E+0	3.80E-1	1.02E-1	1.89E-2	8.24E-1	3.79E-1	1.12E-1	2.18E-2
5.09E-1	2.62E-1	9.87E-2	3.12E-2	8.41E-1	3.84E-1	1.40E-1	4.54E-2	1.11E-2	7.57E-1
3.79E-1	1.63E-1	5.75E-2	1.62E-2	3.44E-3	3.08E-1	1.23E-1	2.65E-2	2.71E-1	2.51E-1
6.08E-2	3.08E-1	5.66E-1	4.49E-1	1.10E-1	3.66E-1	6.53E-1	3.25E-1	1.09E-1	2.91E-1
4.47E-1	3.25E-1	1.24E-1	2.63E-1	2.73E-1	1.58E-1	6.82E-2	2.93E-1	4.70E-1	2.83E-1
1.33E-1	5.11E-2	2.75E-1	2.94E-1	2.57E-1	1.70E-1	8.31E-2	2.76E-2	1.64E-1	1.19E-1
8.24E-2	1.17E-1	2.01E-1	1.19E-1	2.61E-2	3.39E-1	3.57E-1	3.77E-1	9.65E-2	3.14E-1
4.50E-1	2.57E-1	7.31E-2	2.67E-1	3.10E-1	2.74E-1	1.33E-1	1.97E-1	1.73E-1	9.13E-2
9.95E-2	2.34E-1	3.03E-1	2.18E-1	9.56E-2	5.94E-2	1.97E-1	1.90E-1	1.66E-1	1.34E-1
7.76E-2	7.29E-2	1.05E-1	9.51E-2	4.77E-2	1.12E-1	1.29E-1	4.21E-3	2.70E-2	2.65E-1
4.44E-1	1.85E-2	1.07E-1	2.56E-1	3.72E-1	1.09E-2	8.05E-2	2.21E-1	3.01E-1	5.88E-2
1.18E-1	1.33E-1	9.07E-2	2.64E-2	1.00E-1	1.67E-1	1.97E-1	1.37E-1	8.28E-3	5.28E-2
1.27E-1	1.54E-1	1.31E-1	7.30E-2	2.42E-2	7.91E-2	7.84E-2	3.35E-1	1.38E-1	3.26E-2
5.95E-1	3.11E-1	1.39E-1	3.76E-2	4.44E-1	2.35E-1	1.17E-1	5.47E-2	5.28E-1	2.84E-1
1.30E-1	5.01E-2	4.10E-1	2.67E-1	1.54E-1	6.52E-2	2.96E+0	1.38E+0	4.41E-1	1.21E-1
3.25E-2	4.33E+0	1.48E+0	4.53E-1	1.29E-1	4.03E-2	1.36E-2	1.99E+0	2.95E-1	4.03E-2
1.84E-1	1.19E-1	7.75E-2	2.09E-1	2.50E-1	2.03E-1	1.56E-1	2.01E-1	2.01E-1	1.51E-1
9.00E-2	2.02E-1	2.52E-1	1.94E-1	1.27E-1	2.30E-1	2.74E-1	1.44E-1	6.87E-2	7.12E-1
1.56E+0	1.15E+0	5.24E-1	1.35E-1	2.03E-1	2.20E+0	1.52E+0	6.67E-1	2.09E-1	4.72E-2
4.94E-1	1.03E+0	2.21E-1	8.43E-2	1.03E-1	6.59E-2	5.23E-2	1.25E-1	1.88E-1	1.78E-1
8.38E-2	1.24E-1	1.23E-1	9.87E-2	6.66E-2	1.32E-1	1.71E-1	1.52E-1	1.37E-1	1.44E-1
1.46E-1	5.98E-2	1.27E-1	7.22E-1	8.25E-1	7.08E-1	4.15E-1	5.47E-2	1.29E-1	1.03E+0
1.11E+0	6.60E-1	2.30E-1	8.48E-2	5.17E-1	5.53E-1	2.90E-2	6.24E-2	3.50E-2	1.01E-3
5.67E-2	9.08E-2	1.23E-1	3.01E-2	5.24E-2	6.90E-2	6.28E-2	1.43E-2	5.41E-2	8.54E-2
1.06E-1	6.50E-2	6.87E-2	5.98E-2	5.31E-2	3.40E-2	9.72E-2	4.19E-1	5.12E-1	3.34E-1
1.65E-2	3.36E-2	6.78E-2	3.94E-1	6.26E-1	4.69E-1	1.46E-2	9.74E-2	4.60E-1	3.62E+0
2.56E-1	8.21E-2	8.44E-2	4.74E-2	2.55E-2	1.37E-2	5.06E-1	2.61E-1	1.25E-1	5.56E-2
1.62E-1	1.14E-1	6.88E-2	3.57E-2	7.37E-1	4.84E-1	2.46E-1	8.78E-2	4.43E-1	3.29E-1
1.89E-1	9.30E-2	3.58E-2	3.85E-1	2.94E-1	1.93E-1	1.08E-1	5.05E-2	1.76E-2	3.21E-1
1.97E-1	6.60E-2	2.56E-1	2.25E+0	1.39E-1	1.84E-2	3.74E-2	3.46E-2	2.40E-2	1.22E-1
2.30E-1	1.84E-1	1.04E-1	7.45E-2	6.02E-2	6.20E-2	6.16E-2	3.81E-1	2.91E-1	2.54E-1
1.58E-1	1.94E-1	1.76E-1	1.65E-1	1.37E-1	7.68E-2	2.09E-1	1.00E-1	9.90E-2	1.17E-1
1.09E-1	6.47E-2	1.68E-1	7.56E-2	1.45E-1	8.19E-2	1.39E-1	1.10E+0	5.47E-3	9.72E-3
1.75E-2	2.37E-2	3.54E-2	6.40E-2	1.05E-1	1.12E-1	1.60E-2	4.07E-2	4.14E-2	3.18E-2
9.60E-2	2.00E-1	1.54E-1	7.51E-2	4.06E-2	1.13E-1	1.09E-1	7.75E-2	3.88E-2	5.30E-3
1.05E-1	1.08E-1	7.50E-2	4.00E-2	1.56E-2	3.04E-2	1.16E-1	4.77E-2		

Table 5. Maxwellian-averaged collision strengths Υ at $T = 20\,000$ K in Fe II

2.91E-1	9.08E-2	8.07E-3	6.37E-1	3.14E-1	9.69E-2	1.71E-2	4.27E-1	2.17E-1	1.14E-1
3.88E-2	4.32E-1	2.26E-1	8.31E-2	1.97E-2	2.88E-1	1.59E-1	7.60E-2	3.86E-2	2.57E+1
6.95E+0	5.84E-1	2.26E-1	8.39E-2	3.17E+1	5.47E+0	5.97E-1	5.97E-2	2.46E-2	1.13E-2
1.41E+1	1.78E-1	4.25E-2	1.38E+0	2.48E-1	9.97E-3	2.02E-3	2.24E+0	2.86E-1	3.04E-2
1.00E-2	8.34E-1	1.47E-2	7.85E-3	1.40E-1	1.02E-1	4.44E-2	1.05E-2	8.03E-2	5.36E-2
2.21E-2	1.66E-1	9.57E-2	5.14E-2	2.83E-1	2.29E-1	2.44E-1	1.01E-1	2.22E-1	2.30E-1
1.03E-1	9.49E-2	1.89E-1	2.27E-1	1.52E-1	8.13E-2	1.80E-1	1.38E-1	1.08E-1	2.90E-2
6.35E+0	1.18E+1	8.68E+0	5.67E-1	1.65E-1	5.23E-1	2.13E+1	7.59E+0	1.18E+0	7.42E-2
1.33E-2	4.13E+0	7.18E+0	1.10E-1	4.57E-1	6.11E-1	2.37E-1	8.02E-3	4.36E-1	1.30E+0
2.90E-1	2.57E-2	3.17E-1	3.63E-1	5.71E-3	1.03E-1	4.08E-2	5.22E-2	4.13E-2	6.43E-2
3.72E-2	2.32E-2	8.31E-2	9.18E-2	6.06E-2	8.11E-2	2.11E-1	1.55E-1	1.96E-1	1.23E-1
1.23E-1	1.66E-1	8.08E-2	7.71E-2	1.49E-1	1.58E-1	1.24E-1	1.07E-1	1.23E-1	6.44E-2
4.95E-2	3.98E-1	8.46E+0	3.91E+0	7.76E+0	3.93E-1	6.28E-2	5.40E-1	1.34E+1	7.53E+0
1.52E+0	7.39E-2	7.66E-1	5.12E+0	2.67E+0	1.12E-1	4.22E-1	3.12E-1	1.37E-1	5.75E-2
5.21E-1	7.76E-1	1.85E-1	1.01E-1	2.95E-1	1.18E-1	5.23E-2	4.68E-2	3.64E-2	4.27E-2
4.63E-2	2.99E-2	1.74E-2	3.45E-2	7.33E-2	4.91E-2	1.25E-2	1.04E-1	1.36E-1	1.76E-1
5.55E-2	8.23E-2	1.10E-1	8.06E-2	2.30E-2	7.72E-2	1.16E-1	1.24E-1	6.33E-2	7.27E-2
5.60E-2	3.82E-2	1.21E-1	5.19E-1	7.62E+0	7.58E-1	4.98E+0	2.84E-2	5.13E-2	3.97E-1
7.57E+0	6.05E+0	1.36E+0	5.21E-2	1.73E+0	3.91E+0	1.75E-2	1.65E-1	2.69E-1	1.99E-1
1.06E-2	8.67E-2	4.62E-1	4.59E-1	2.70E-2	1.42E-1	1.73E-1	1.87E-2	4.17E-2	3.38E-2
2.45E-2	2.92E-2	2.27E-2	1.05E-2	1.08E-2	4.06E-2	2.69E-2	9.57E-4	1.91E-2	9.96E-2
9.47E-2	1.70E-2	5.38E-2	3.63E-2	5.74E-2	3.88E-3	3.04E-2	5.88E-2	7.71E-2	3.09E-2
2.63E-2	4.14E-2	1.65E-2	3.35E-2	1.65E-1	3.93E-1	4.96E+0	1.53E+0	1.35E-2	1.28E-2
3.06E-2	2.20E-1	3.39E+0	4.07E+0	1.70E-2	5.71E-2	2.78E+0	2.09E-3	2.85E-2	1.53E-1
1.41E-1	4.94E-3	5.37E-3	8.67E-2	4.11E-1	6.26E-3	4.18E-2	1.23E-1	4.01E-3	2.30E-2
2.41E-2	8.16E-3	1.40E-2	1.25E-2	4.65E-3	6.15E-1	1.30E-1	3.44E-2	1.51E+0	5.44E-1
1.39E-1	3.06E-2	1.60E+0	4.91E-1	1.41E-1	3.71E-2	1.16E+0	4.87E-1	1.54E-1	4.20E-2
8.74E-1	4.01E-1	1.67E-1	6.11E-2	7.59E-1	3.35E-1	1.23E-1	3.92E-2	9.01E-3	7.17E-1
3.57E-1	1.53E-1	5.34E-2	1.47E-2	2.96E-3	2.71E-1	1.10E-1	2.34E-2	2.93E-1	2.65E-1
6.80E-2	3.92E-1	7.64E-1	5.36E-1	1.53E-1	4.82E-1	8.45E-1	4.06E-1	1.38E-1	3.91E-1
5.97E-1	4.10E-1	1.59E-1	4.46E-1	4.31E-1	2.44E-1	1.02E-1	2.72E-1	3.87E-1	2.41E-1
1.17E-1	4.55E-2	2.59E-1	2.77E-1	2.43E-1	1.60E-1	7.81E-2	2.57E-2	1.46E-1	1.03E-1
7.43E-2	1.30E-1	2.13E-1	1.25E-1	5.51E-2	3.92E-1	5.01E-1	4.50E-1	1.38E-1	3.99E-1
5.65E-1	3.15E-1	1.07E-1	3.40E-1	4.05E-1	3.41E-1	2.27E-1	3.05E-1	2.62E-1	1.35E-1
9.07E-2	2.03E-1	2.51E-1	1.83E-1	8.41E-2	5.46E-2	1.86E-1	1.80E-1	1.57E-1	1.27E-1
7.37E-2	6.52E-2	9.25E-2	8.43E-2	5.55E-2	1.21E-1	1.34E-1	1.30E-2	5.35E-2	3.09E-1
5.62E-1	3.69E-2	1.37E-1	3.14E-1	4.61E-1	2.60E-2	1.05E-1	2.74E-1	3.88E-1	1.10E-1
1.76E-1	1.99E-1	1.37E-1	2.23E-2	8.88E-2	1.46E-1	1.67E-1	1.13E-1	7.12E-3	4.89E-2
1.20E-1	1.46E-1	1.24E-1	6.95E-2	2.14E-2	7.12E-2	6.84E-2	3.38E-1	1.36E-1	3.22E-2
5.47E-1	2.85E-1	1.27E-1	3.49E-2	4.62E-1	2.37E-1	1.17E-1	5.36E-2	5.00E-1	2.58E-1
1.16E-1	4.49E-2	3.88E-1	2.25E-1	1.27E-1	5.66E-2	2.58E+0	1.08E+0	3.24E-1	8.09E-2
2.01E-2	3.56E+0	1.19E+0	3.47E-1	9.25E-2	2.70E-2	9.06E-3	1.69E+0	2.37E-1	2.83E-2
1.83E-1	1.22E-1	7.58E-2	1.92E-1	2.28E-1	1.89E-1	1.41E-1	2.01E-1	2.11E-1	1.52E-1
9.13E-2	1.83E-1	2.35E-1	1.79E-1	1.13E-1	2.04E-1	2.36E-1	1.26E-1	5.52E-2	5.70E-1
1.28E+0	9.23E-1	4.06E-1	9.56E-2	1.24E-1	1.82E+0	1.25E+0	5.34E-1	1.58E-1	3.19E-2
4.09E-1	8.78E-1	1.80E-1	8.34E-2	1.04E-1	6.64E-2	4.66E-2	1.19E-1	1.68E-1	1.65E-1
8.37E-2	1.22E-1	1.32E-1	1.00E-1	5.90E-2	1.20E-1	1.57E-1	1.40E-1	1.19E-1	1.26E-1
1.21E-1	5.39E-2	7.95E-2	5.65E-1	6.68E-1	5.76E-1	3.35E-1	3.55E-2	7.86E-2	8.51E-1
9.21E-1	5.39E-1	1.82E-1	6.44E-2	4.37E-1	4.72E-1	2.86E-2	6.14E-2	3.63E-2	1.65E-3
4.95E-2	8.48E-2	1.12E-1	2.92E-2	5.36E-2	6.83E-2	6.75E-2	1.31E-2	4.72E-2	7.78E-2
9.94E-2	5.65E-2	5.52E-2	5.39E-2	4.56E-2	2.09E-2	6.08E-2	3.28E-1	4.20E-1	2.80E-1
1.14E-2	2.12E-2	4.10E-2	3.17E-1	5.18E-1	3.93E-1	9.60E-3	7.76E-2	3.96E-1	3.65E+0
2.81E-1	8.44E-2	1.44E-1	8.01E-2	4.27E-2	2.23E-2	6.02E-1	3.02E-1	1.43E-1	6.40E-2
1.92E-1	1.30E-1	7.83E-2	4.16E-2	7.32E-1	4.61E-1	2.29E-1	8.21E-2	3.52E-1	2.51E-1
1.43E-1	6.99E-2	2.66E-2	3.18E-1	2.45E-1	1.61E-1	8.99E-2	4.17E-2	1.45E-2	2.72E-1
1.67E-1	5.59E-2	2.81E-1	2.24E+0	1.59E-1	3.00E-2	6.39E-2	5.88E-2	4.03E-2	1.39E-1
2.74E-1	2.15E-1	1.19E-1	8.29E-2	7.31E-2	7.29E-2	6.86E-2	3.62E-1	2.70E-1	2.43E-1
1.53E-1	1.53E-1	1.32E-1	1.25E-1	1.04E-1	5.91E-2	1.75E-1	8.14E-2	8.07E-2	9.65E-2
9.11E-2	5.44E-2	1.42E-1	6.40E-2	1.23E-1	8.42E-2	1.59E-1	1.09E+0	8.91E-3	1.63E-2
2.95E-2	4.05E-2	4.18E-2	7.15E-2	1.23E-1	1.34E-1	1.93E-2	4.44E-2	4.70E-2	3.84E-2
9.16E-2	1.95E-1	1.47E-1	7.07E-2	2.97E-2	8.66E-2	8.35E-2	5.93E-2	2.95E-2	3.71E-3
8.81E-2	9.01E-2	6.21E-2	3.26E-2	1.25E-2	2.58E-2	9.86E-2	4.04E-2		

Table 6. Maxwellian-averaged collision strengths Υ at $T = 50\,000$ K in Fe II

2.73E-1	7.91E-2	6.40E-3	6.58E-1	3.23E-1	9.89E-2	1.70E-2	4.36E-1	2.15E-1	1.15E-1
3.89E-2	5.02E-1	2.36E-1	8.60E-2	1.93E-2	2.93E-1	1.63E-1	7.92E-2	4.08E-2	3.34E+1
8.36E+0	3.10E-1	1.01E-1	3.66E-2	3.90E+1	6.86E+0	6.94E-1	5.05E-2	2.22E-2	1.05E-2
1.90E+1	1.55E-1	3.83E-2	1.22E+0	2.16E-1	6.99E-3	1.50E-3	1.94E+0	2.45E-1	2.61E-2
8.89E-3	7.58E-1	1.16E-2	6.12E-3	1.65E-1	1.23E-1	5.32E-2	1.23E-2	9.29E-2	6.48E-2
2.74E-2	1.52E-1	9.06E-2	4.50E-2	2.92E-1	2.33E-1	2.51E-1	1.03E-1	2.26E-1	2.29E-1
9.93E-2	9.56E-2	2.16E-1	2.32E-1	1.58E-1	8.51E-2	1.86E-1	1.37E-1	1.11E-1	2.95E-2
7.64E+0	1.50E+1	1.11E+1	3.33E-1	7.61E-2	4.29E-1	2.71E+1	9.81E+0	1.44E+0	6.01E-2
1.08E-2	5.44E+0	9.74E+0	9.63E-2	4.01E-1	5.41E-1	2.08E-1	5.51E-3	3.76E-1	1.13E+0
2.50E-1	2.18E-2	2.87E-1	3.30E-1	4.51E-3	1.24E-1	4.51E-2	6.24E-2	4.99E-2	7.48E-2
4.42E-2	2.71E-2	7.41E-2	8.61E-2	5.54E-2	8.29E-2	2.18E-1	1.58E-1	2.02E-1	1.24E-1
1.20E-1	1.66E-1	7.87E-2	8.26E-2	1.55E-1	1.62E-1	1.29E-1	1.11E-1	1.24E-1	6.25E-2
5.06E-2	2.32E-1	1.05E+1	4.69E+0	1.01E+1	2.47E-1	5.13E-2	4.50E-1	1.75E+1	9.91E+0
1.91E+0	5.90E-2	9.59E-1	6.86E+0	3.59E+0	9.68E-2	3.73E-1	2.75E-1	1.21E-1	4.92E-2
4.50E-1	6.72E-1	1.59E-1	9.07E-2	2.68E-1	1.07E-1	6.28E-2	5.54E-2	4.23E-2	5.13E-2
5.42E-2	3.49E-2	2.02E-2	3.00E-2	6.70E-2	4.66E-2	1.23E-2	1.07E-1	1.39E-1	1.81E-1
5.59E-2	8.16E-2	1.10E-1	7.95E-2	2.32E-2	8.08E-2	1.21E-1	1.29E-1	6.62E-2	7.39E-2
5.50E-2	3.78E-2	5.80E-2	3.12E-1	9.78E+0	6.17E-1	6.51E+0	2.59E-2	3.89E-2	3.34E-1
9.96E+0	8.04E+0	1.73E+0	4.64E-2	2.27E+0	5.26E+0	1.43E-2	1.45E-1	2.39E-1	1.77E-1
9.27E-3	7.42E-2	4.01E-1	3.99E-1	2.35E-2	1.29E-1	1.58E-1	2.23E-2	5.03E-2	4.00E-2
2.87E-2	3.48E-2	2.62E-2	1.18E-2	9.17E-3	3.65E-2	2.61E-2	8.00E-4	1.92E-2	1.03E-1
9.69E-2	1.70E-2	5.44E-2	3.47E-2	5.73E-2	3.44E-3	3.19E-2	6.18E-2	7.91E-2	3.25E-2
2.66E-2	4.18E-2	1.54E-2	1.60E-2	7.60E-2	2.46E-1	6.41E+0	1.94E+0	1.26E-2	1.12E-2
2.18E-2	1.84E-1	4.44E+0	5.46E+0	1.53E-2	4.95E-2	3.72E+0	1.52E-3	2.41E-2	1.36E-1
1.26E-1	4.39E-3	4.42E-3	7.47E-2	3.58E-1	5.11E-3	3.78E-2	1.12E-1	4.46E-3	2.78E-2
2.91E-2	8.79E-3	1.74E-2	1.41E-2	5.28E-3	5.94E-1	1.24E-1	3.49E-2	1.76E+0	6.05E-1
1.69E-1	4.54E-2	1.77E+0	5.31E-1	1.62E-1	5.12E-2	1.26E+0	4.95E-1	1.61E-1	5.28E-2
9.31E-1	4.12E-1	1.79E-1	6.94E-2	6.45E-1	2.80E-1	1.03E-1	3.15E-2	6.31E-3	6.19E-1
3.11E-1	1.33E-1	4.58E-2	1.20E-2	2.20E-3	2.26E-1	9.80E-2	1.96E-2	2.82E-1	2.58E-1
6.44E-2	4.31E-1	9.12E-1	5.70E-1	1.80E-1	5.27E-1	9.31E-1	4.31E-1	1.49E-1	4.07E-1
6.31E-1	4.15E-1	1.59E-1	4.74E-1	4.51E-1	2.53E-1	1.03E-1	2.39E-1	3.02E-1	1.94E-1
9.84E-2	3.94E-2	2.27E-1	2.31E-1	2.09E-1	1.40E-1	6.84E-2	2.22E-2	1.26E-1	8.17E-2
6.67E-2	1.26E-1	2.06E-1	1.20E-1	7.98E-2	4.02E-1	6.16E-1	4.77E-1	1.60E-1	4.28E-1
6.15E-1	3.30E-1	1.15E-1	3.47E-1	4.22E-1	3.40E-1	2.43E-1	3.16E-1	2.68E-1	1.38E-1
7.80E-2	1.67E-1	1.98E-1	1.47E-1	7.07E-2	4.58E-2	1.63E-1	1.53E-1	1.34E-1	1.11E-1
6.54E-2	5.71E-2	7.70E-2	7.17E-2	5.48E-2	1.15E-1	1.31E-1	2.17E-2	7.47E-2	3.17E-1
6.39E-1	5.10E-2	1.49E-1	3.29E-1	4.95E-1	3.53E-2	1.05E-1	2.73E-1	4.00E-1	1.22E-1
1.78E-1	2.03E-1	1.41E-1	1.67E-2	7.61E-2	1.23E-1	1.34E-1	8.83E-2	5.28E-3	4.21E-2
1.06E-1	1.28E-1	1.07E-1	5.92E-2	1.81E-2	6.38E-2	5.53E-2	2.63E-1	1.04E-1	2.32E-2
4.05E-1	2.10E-1	9.27E-2	2.58E-2	3.72E-1	1.86E-1	9.09E-2	4.04E-2	3.71E-1	1.83E-1
8.03E-2	3.02E-2	2.87E-1	1.53E-1	8.37E-2	3.79E-2	2.00E+0	7.56E-1	2.09E-1	4.47E-2
9.57E-3	2.71E+0	8.84E-1	2.46E-1	6.02E-2	1.60E-2	5.31E-3	1.34E+0	1.78E-1	1.79E-2
1.41E-1	9.37E-2	5.90E-2	1.41E-1	1.68E-1	1.42E-1	1.02E-1	1.56E-1	1.71E-1	1.18E-1
7.17E-2	1.29E-1	1.71E-1	1.29E-1	7.89E-2	1.44E-1	1.62E-1	8.86E-2	3.62E-2	4.01E-1
9.40E-1	6.68E-1	2.80E-1	5.80E-2	6.29E-2	1.40E+0	9.52E-1	3.97E-1	1.11E-1	1.92E-2
3.15E-1	6.96E-1	1.37E-1	6.30E-2	8.06E-2	5.19E-2	3.29E-2	9.00E-2	1.20E-1	1.23E-1
6.45E-2	9.42E-2	1.08E-1	7.85E-2	3.98E-2	8.57E-2	1.13E-1	1.01E-1	8.00E-2	8.86E-2
8.12E-2	3.96E-2	3.83E-2	3.95E-1	4.86E-1	4.21E-1	2.43E-1	1.98E-2	3.94E-2	6.50E-1
7.07E-1	4.09E-1	1.35E-1	4.53E-2	3.44E-1	3.74E-1	2.10E-2	4.80E-2	2.84E-2	1.74E-3
3.41E-2	6.39E-2	8.26E-2	2.15E-2	4.23E-2	5.29E-2	5.58E-2	8.81E-3	3.19E-2	5.57E-2
7.30E-2	3.79E-2	3.62E-2	3.96E-2	3.16E-2	9.95E-3	2.92E-2	2.30E-1	3.10E-1	2.12E-1
6.92E-3	1.13E-2	2.02E-2	2.36E-1	3.98E-1	3.05E-1	5.49E-3	5.78E-2	3.17E-1	3.55E+0
2.48E-1	7.43E-2	1.73E-1	9.48E-2	4.94E-2	2.48E-2	6.25E-1	2.94E-1	1.31E-1	5.72E-2
1.68E-1	1.08E-1	6.38E-2	3.36E-2	5.80E-1	3.61E-1	1.74E-1	6.03E-2	2.50E-1	1.71E-1
9.83E-2	4.84E-2	1.83E-2	2.52E-1	2.02E-1	1.35E-1	7.63E-2	3.54E-2	1.22E-2	2.27E-1
1.37E-1	4.29E-2	2.48E-1	2.20E+0	1.40E-1	3.32E-2	7.68E-2	7.08E-2	4.76E-2	1.24E-1
2.83E-1	2.20E-1	1.16E-1	6.58E-2	6.46E-2	6.31E-2	5.63E-2	2.84E-1	1.95E-1	1.89E-1
1.25E-1	1.08E-1	9.11E-2	8.60E-2	7.10E-2	4.02E-2	1.53E-1	6.03E-2	5.99E-2	7.78E-2
7.69E-2	4.72E-2	1.16E-1	5.11E-2	1.04E-1	7.42E-2	1.40E-1	1.08E+0	9.63E-3	1.81E-2
3.53E-2	4.99E-2	3.69E-2	6.38E-2	1.25E-1	1.43E-1	1.56E-2	3.50E-2	3.96E-2	3.48E-2
6.63E-2	1.60E-1	1.16E-1	5.17E-2	2.17E-2	5.87E-2	5.70E-2	4.08E-2	2.05E-2	2.16E-3
7.75E-2	7.67E-2	4.98E-2	2.36E-2	7.75E-3	1.85E-2	8.29E-2	3.42E-2		

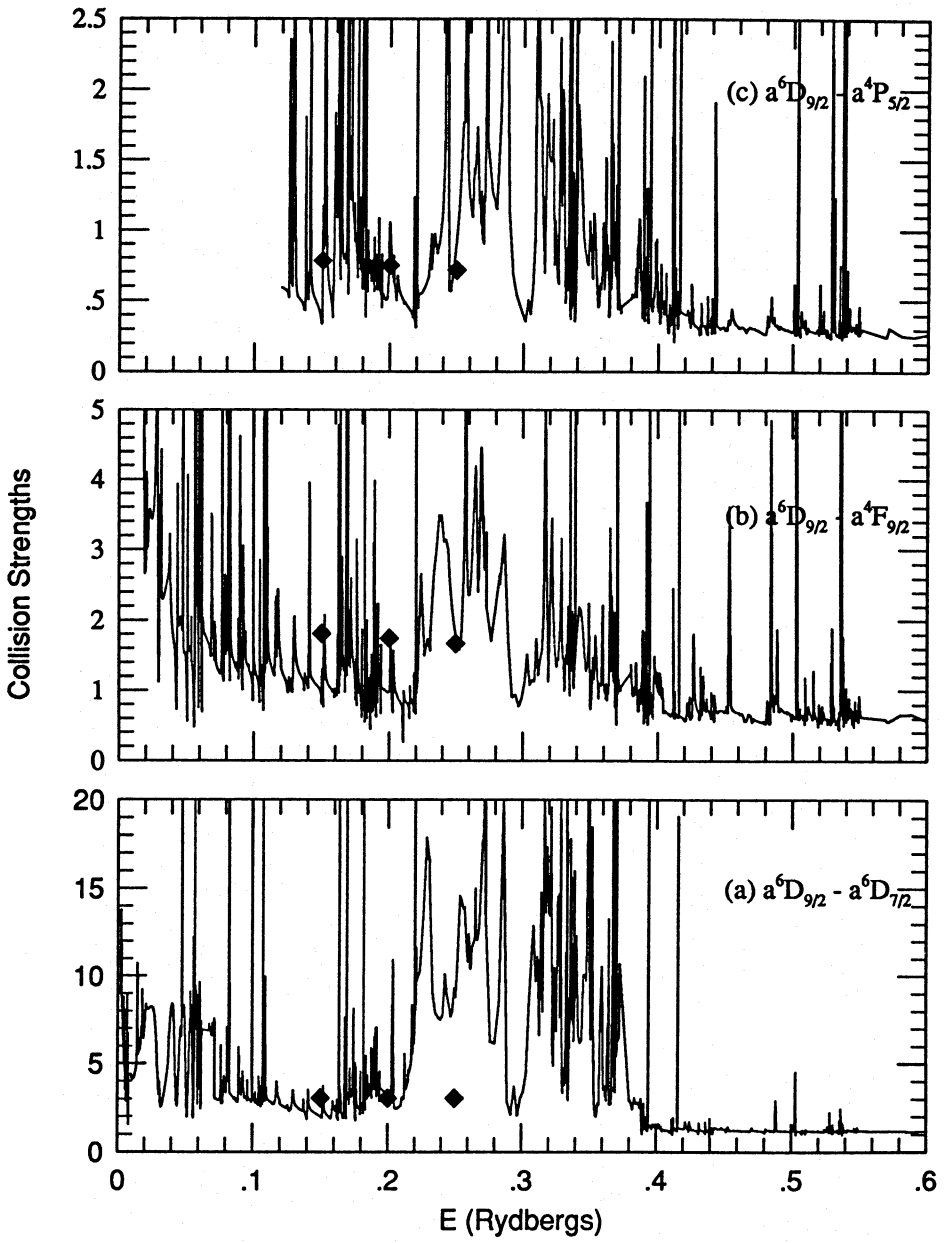

Fig. 1a–c. The collision strengths for the forbidden transitions $a^6D_{9/2} - a^6D_{7/2}$ (**a**); $a^6D_{9/2} - a^4F_{9/2}$ (**b**) and $a^6D_{9/2} - a^4P_{5/2}$ (**c**). The diamond-shaped dots represent the NS (1980) values

so that the latter effects could be neglected in order to emphasize the former effects.

First, we study the forbidden transitions from the ground level $a^6D_{9/2}$ to some low-lying levels, for example, to $a^6D_{7/2}$, $a^4F_{9/2}$ and $a^4P_{5/2}$. The present collision strengths, as well as those by NS in diamond-shaped dots, for these transitions are plotted in Fig. 1. From comparison with the NS results, one would expect that the resonances would enhance the rate coefficients considerably, as pointed out by PB and as shown in the next section. Figure 1b and 1c are very similar to Fig. 1a and 1c in PB as expected, but the former have much more resonance structures than in corresponding Fig. 6 in PB, which shows the BP results with 41-level calculations. This again indicates that the amount of coupling included in the BP calculations by PB is inadequate and the redistribution of scattering flux into excited states is not fully taken into account (as pointed out in PB).

The excitation of metastable levels, such as those of a^4F and a^4D, is of great interest in the study of astrophysical sources. Figure 2 shows collision strengths for transitions $a^4F_{9/2} - a^4D_{7/2}$ (a), $a^4F_{9/2} - a^4P_{5/2}$ (b), and $a^4D_{7/2} - a^4P_{5/2}$ (c). Again the diamond-shaped dots indicate the NS values. For these transitions the resonance structure would also enhance the rate coefficients considerably. In Fig. 2b the NS values, being larger than the present results, are rising rapidly with energies, which is difficult to explain. This transition is one of the rare cases where the NS collision strength for $E = 0.2$ Ryd is larger than the present effective collision strengths at $T = 3000$ K as shown in Table 7.

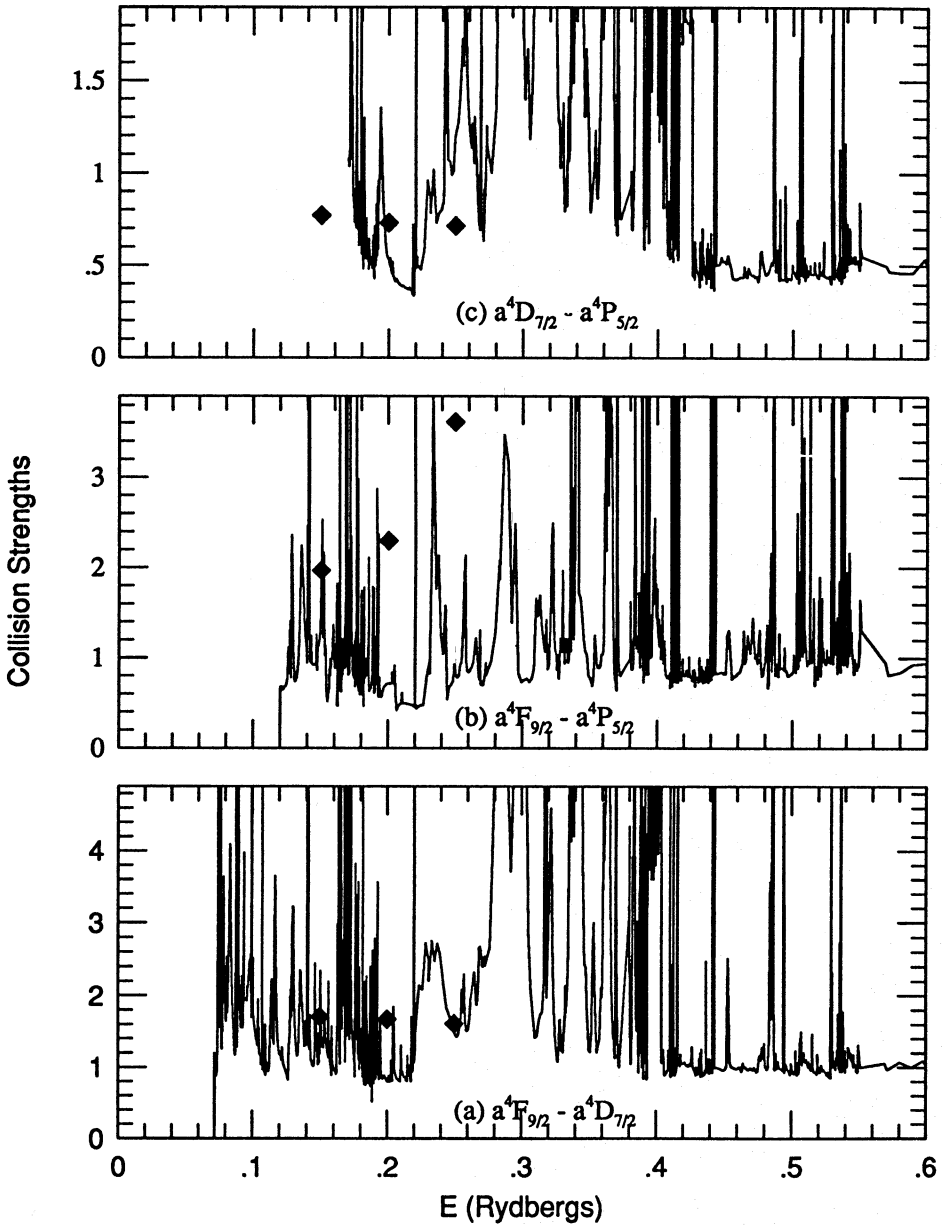

Fig. 2a–c. The collision strengths for the transitions between the metastable levels, $a^4F_{9/2} - a^4D_{7/2}$ (**a**); $a^4F_{9/2} - a^4P_{5/2}$ (**b**) and $a^4D_{7/2} - a^4P_{5/2}$ (**c**). The diamond-shaped dots represent the NS (1980) values

Figure 3 shows the collision strengths for optically allowed transitions $a^6D_{9/2} - z^6D^o_{9/2}$ (a), $a^6D_{9/2} - z^6F^o_{11/2}$ (b), and $a^6D_{9/2} - z^6P^o_{7/2}$ (c). As we mentioned earlier, the Coulomb-Bethe approximation was employed to estimate the contributions by higher partial waves and the resultant total collision strengths were summed over the total target level angular momenta J_t's to match with the LS coupling collision strengths between the energy terms. It is obvious from the figure that the shape of the present collision strengths is similar to that in Fig. 2 of PB. Resonances are not as strong as in the allowed transitions and the rate coefficients will be dominated by the high energy region.

3. Rate coefficients

The maxwellian averaged collision strength, also known as the effective collision strength, is given by

$$\Upsilon_{ij} = \int_0^\infty \Omega_{ij} e^{-\epsilon_j/kT} d(\epsilon_j/kT)\,. \tag{1}$$

Here Ω_{ij}, the collision strength for excitation from level i to level j, is averaged over a maxwellian distribution of incident electron energies ϵ_j above the excitation threshold of the level j, at temperature T. This slowly varying function of temperature can then be used to obtain the rate coefficient, q_{ij}, for electron impact excitation,

$$q_{ij} = \frac{8.63\text{x}10^{-6}}{\sqrt{T}\,g_i} e^{-E_{ij}/kT} \Upsilon_{ij} \quad (\text{cm}^3\,\text{s}^{-1}), \tag{2}$$

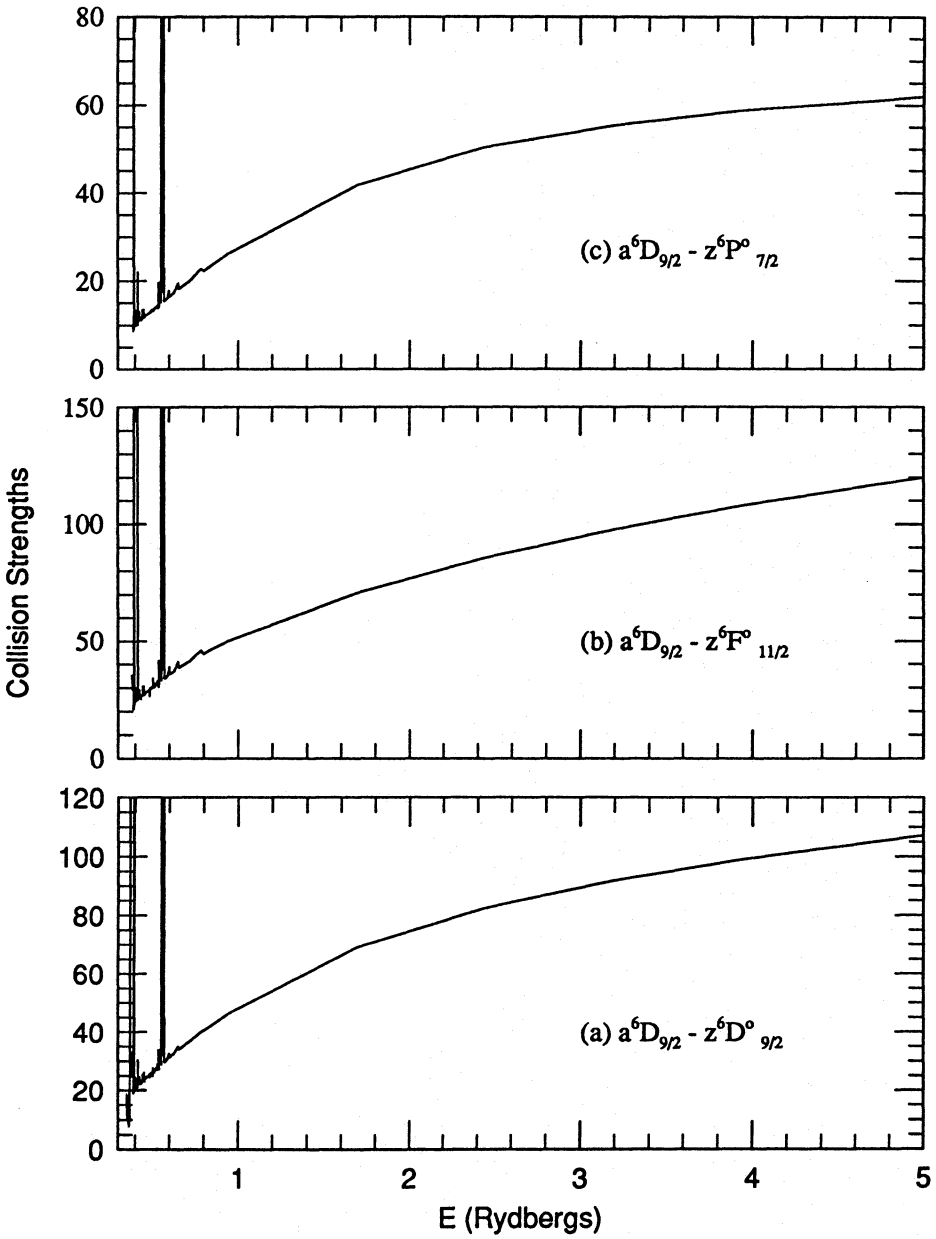

Fig. 3a–c. The collision strengths for the allowed transitions from the ground level, $a^6D_{9/2} - z^6D^o_{9/2}$ (**a**); $a^6D_{9/2} - z^6F^o_{11/2}$ (**b**) and $a^6D_{9/2} - z^6P^o_{7/2}$ (**c**)

where E_{ij} is the energy difference between levels i and j and g_i is the statistical weight of level i.

Although we have carried out the calculations of maxwellian averaged collision strengths for all 10 011 transitions between 142 energy levels shown in Table 1 for 20 temperatures ranging from 1000 to 100 000 K, in the present paper we present only sample results for some transitions at 4 temperatures, 5000, 10 000, 20 000 and 50 000 K. It is noted that sample results of rate coefficients for transitions between the lowest 16 levels in Table 1 were given in Pradhan & Zhang (1993) and are not presented here. The entire set of data is available electronically on Internet by writing to the authors at: zhang@payne.mps.ohio-state.edu.

In Table 2 the transition key index is given for the sample rate coefficients tabulated in this paper. There are 618 pairs of initial and the final levels for the 618 transitions included. These level indices refer to energy level indices in Table 1. The rate coefficients (or more precisely the maxwellian-averaged collision strengths) for these transitions at the 4 temperatures are given in Table 3–6, with one table for each temperature.

Similar to the earlier works in the Iron Project series, (e.g. Paper III; Zhang et al. 1994), the calculations for the effective collision strengths are divided into two parts, one from the contribution from the finer $\nu-$mesh below 0.55 Ryd (as explained in Sect. 2), and the other from a coarser energy mesh above this energy. Also as mentioned before, we included contributions to the collision strength from partial waves with J range 0–6 for $E \leq 0.349$ and with J range 0–10 for $E > 0.349$. In the latter case the collision strengths are in 2 parts, (i) $0 \leq J \leq 6$, and (ii) $7 \leq J \leq 10$. It was found that part (ii) contained

Table 7. Comparison of rate coefficients, the entries with "NS: $\Omega(E = 0.2)$" represent the collision strengths at $E = 0.2$ Ryd in NS (1980); "Keenan" represents the rate coefficients in Keenan et al. (1988); and "4 CC" represents rate coefficients calculated with a 4-term expansion

Transition	NS: Ω(E=0.2)	Keenan	4 CC	Present
$a^6D_{9/2} - a^6D_{7/2}$	3.046	3.460	2.880	6.269
$a^6D_{9/2} - a^6D_{5/2}$	0.922	0.728	0.551	1.853
$a^6D_{9/2} - a^6D_{3/2}$	0.628	0.388	0.223	0.860
$a^6D_{9/2} - a^6D_{1/2}$	0.322	0.193	0.098	0.360
$a^6D_{9/2} - a^4F_{9/2}$	1.742	2.640	2.278	4.004
$a^6D_{9/2} - a^4F_{7/2}$	0.638	0.891	0.834	1.704
$a^6D_{9/2} - a^4F_{5/2}$	0.109	0.159	0.155	0.591
$a^6D_{9/2} - a^4F_{3/2}$	0.008	0.020	0.015	0.165
$a^6D_{7/2} - a^6D_{5/2}$	3.293	3.670	3.044	5.803
$a^6D_{7/2} - a^6D_{3/2}$	0.497	0.518	0.508	1.423
$a^6D_{7/2} - a^6D_{1/2}$	0.229	0.160	0.124	0.527
$a^6D_{7/2} - a^4F_{9/2}$	0.714	1.250	0.933	1.839
$a^6D_{7/2} - a^4F_{7/2}$	0.620	0.966	0.830	1.673
$a^6D_{7/2} - a^4F_{5/2}$	0.545	0.765	0.701	1.119
$a^6D_{7/2} - a^4F_{3/2}$	0.119	0.169	0.163	0.529
$a^6D_{5/2} - a^6D_{3/2}$	2.713	3.080	2.454	4.547
$a^6D_{5/2} - a^6D_{1/2}$	0.191	0.286	0.353	0.854
$a^6D_{5/2} - a^4F_{9/2}$	0.192	0.444	0.260	0.743
$a^6D_{5/2} - a^4F_{7/2}$	0.567	0.882	0.735	1.219
$a^6D_{5/2} - a^4F_{5/2}$	0.361	0.575	0.488	1.097
$a^6D_{5/2} - a^4F_{3/2}$	0.378	0.543	0.487	0.813
$a^6D_{3/2} - a^6D_{1/2}$	1.652	1.920	1.554	2.739
$a^6D_{3/2} - a^4F_{9/2}$	0.026	0.122	0.041	0.254
$a^6D_{3/2} - a^4F_{7/2}$	0.269	0.464	0.350	0.683
$a^6D_{3/2} - a^4F_{5/2}$	0.336	0.512	0.444	0.861
$a^6D_{3/2} - a^4F_{3/2}$	0.367	0.549	0.477	0.786
$a^6D_{1/2} - a^4F_{9/2}$	0.001	0.037	0.004	0.070
$a^6D_{1/2} - a^4F_{7/2}$	0.046	0.088	0.065	0.270
$a^6D_{1/2} - a^4F_{5/2}$	0.253	0.364	0.323	0.483
$a^6D_{1/2} - a^4F_{3/2}$	0.199	0.277	0.263	0.472
$a^4F_{9/2} - a^4F_{7/2}$	3.405	3.270	1.265	8.804
$a^4F_{9/2} - a^4F_{5/2}$	1.229	0.949	0.374	2.357
$a^4F_{9/2} - a^4F_{3/2}$	0.400	0.309	0.123	0.655
$a^4F_{7/2} - a^4F_{5/2}$	2.450	2.570	1.042	7.601
$a^4F_{7/2} - a^4F_{3/2}$	1.125	0.756	0.341	2.279
$a^4F_{5/2} - a^4F_{3/2}$	1.882	1.860	0.793	5.853

pseudo-resonances for about 100 forbidden transitions and a few weak optically allowed transitions (the oscillator strengths or line strengths we used for the Coulomb-Bethe approximation are very weak for these allowed transitions). We employed approximate numerical procedures to detect and smooth over the pseudo-resonances in the code that carries out the maxwellian average. The treatment for Fe II is much more extensive than similar procedures used in Paper III.

4. Discussion

In this section we give an estimate of the accuracy of the present data and a comparison of the present results with those in earlier works.

The fine $\nu-$mesh below $E = 0.55$ Ryd, for excitation of the lower-lying, even-parity levels, fully resolved the important resonance features associated not only with the sextet odd-parity levels z^6D^o, z^6F^o and z^6P^o, but also with the higher z^4D^o, z^4F^o and z^4P^o quartet levels. Therefore, rate coefficients for this type of transitions should be highly accurate, $\approx$ 10–20%. For optically allowed transitions from the a^6D_J levels to the fine structure levels of the z^6D^o, z^6F^o and z^6P^o, the rate coefficients should also be of the same accuracy since resonances are relatively less important and the collision strengths are large and dominated by the higher partial waves. For excitation to intermediate energy levels, up to those of the c^4P term, and transitions between these levels, the accuracy of the rate coefficients is expected to be less, $\approx$ 30–50%. As for the transitions of excitation to the high-lying levels, those with threshold energies greater than 0.55 Ryd, since an energy mesh was used and the resonances and coupling effects due to higher terms and due to other high-energy terms not included in the present calculations were omitted, the uncertainty could exceed 50%.

In Table 7 we make a comparison of the present effective collision strengths, Υ, for some transitions between the lowest 16 levels at $T = 3000$ K with those by Keenan et al. (1988). The collision strengths for $E = 0.2$ Ryd in NS (1980) are also listed since they would roughly indicate their Υ-values at $T = 3000$ K. The present values are generally higher than the previous results, which is mainly due to more resonances and coupling effects included in the present work. This is borne out by another calculation that we carried out as a check with the same 4-term target expansion a^6D, a^4F, a^4D and a^4P. Rate coefficients obtained with this calculation (4CC) are also included in the table. We see that the present 4CC results are generally in good agreement with the previous NS and Keenan et al. (1988) results.

5. Conclusion

Atomic data for Fe II is very important as is pointed out in Sect. 1. The present work has provided a much more extensive and accurate set of collisional data for Fe II, than is currently available. Work is in progress on an even larger set of calculations that would include additional excited sextet and doublet terms and the associated fine structure levels. However, the intensive computational requirements make it difficult to set a time limit for completion. The new work is not expected to significantly alter most of the present data, with the exception of that involving the high-lying terms of the $3d^64p$ configuration.

Acknowledgements. This work was supported partially by the U.S. National Science Foundation (PHY-9115057) and NASA LTSA program (NAGW-3315). The computational work was carried out on the Cray Y-MP8/64 at the Ohio Supercomputer Center in Columbus, Ohio.

References

Baluja K.L., Hibbert A., Mohan M., 1986, J. Phys. B 19, 3613

Berrington K.A., Burke P.G., Hibbert A., Mohan M., Baluja K.L., 1988, J. Phys. B 21, 339

Corliss C., Sugar J., 1982, J. Phys. Chem. Ref. Data 11, 135

Eissner W., Jones M., Nussbaumer H., 1974, Comput. Phys. Commun. 8, 270

Hummer D.G., Berrington K.A., Eissner W., et al., 1993, A&A 279, 298 (Paper I)

Keenan F.P, Hibbert A., Burke P.G., Berrington K.A., 1988, ApJ 332, 539

Nahar S.N., 1994, A&A (the accompanying paper, Paper VII)

Nahar S.N., Pradhan A.K., 1994 J. Phys. B 27, 429

Nussbaumer H., Storey P.J., 1980, A&A 89, 308 (NS 1980)

Nussbaumer H., Storey P.J., 1988, A&A 193, 327 (NS 1988)

Pradhan A.K., Berrington K.A., 1993 J. Phys. B 26, 157 (PB)

Pradhan A.K., Zhang H.L., 1993, ApJ 409, L77

Seaton M.J., 1975, Advances in Atomic and Molecular Physics, Vol. 11, Academic Press, Inc., p. 83

Viotti R., Vittone A., Friedjung M. (eds.), 1988, IAU Colloquium 94, Physics of Formation of Fe II Lines outside LTE. Reidel, Dordrecht

Zhang H.L., Graziani M., Pradhan A.K., 1994, A&A 283, 319 (Paper III)